Vol. 03, Iss. 3 (2025) 301-313, DOI: 10.61552/JME.2025.03.005

JME

Journal of Materials and Engineering

www.jme.aspur.rs

Research article

Evaluating Thermal and Dielectric Properties of Wax Patterns and Their Effects on Ceramic Mould During the Microwave Dewaxing Process

Ahmed Omar Aswaye Amhamed[a,b], Wan Fahmin Faiz Wan Ali[a,*], Izman Sudin[a], Najlaa Nazihah Binti Mas'ood[a], Najib Meftah Almukhtar Omar[c], Mohd Azlan bin Suhaimi[a]

[a]*Faculty of Mechanical Engineering, Universiti Teknologi Malaysia, 81310 UTM, Skudai, Johor Bahru, Malaysia,*
[b]*Mechanical Engineering Department, Sabratha Faculty of Engineering, Sabratha University, Libya,*
[c]*Chemical Engineering Department, Sabratha Faculty of Engineering, Sabratha University, Libya.*

Keywords:

Investment casting
Microwave heating
Dielectric properties
Dewaxing
Crack

* Corresponding author:

Wan Fahmin Faiz Wan Ali
E-mail: wan_fahmin@utm.my

Received: 18 August 2024
Revised: 20 September 2024
Accepted: 11 October 2024

A B S T R A C T

Dewaxing process in investment casting (IC) encounters multiple challenges such as high energy consumption, mould cracking, and wax contamination. One of the contributors to mould cracks is the disparity in thermal properties between the wax pattern and green ceramic mould, which leads to defective castings. This study aims to compare the thermal and dielectric properties of the commercial investment casting wax HYFILL B289 MOD S and a new wax SIVUCH L1203 and their effects on the ceramic mould during the microwave dewaxing process. TGA and DTA analyses were conducted on both waxes, while dielectric properties were evaluated on waxes and the green ceramic mould. Additionally, the strength of the green moulds was tested. The results indicated that SIVUCH L1203 wax outperformed its counterpart, HYFILL B289 MOD S wax, owing to its thermal and absorbing properties, which are superior to meeting investment casting requirements. Specifically, SIVUCH L1203 wax demonstrated an impeccably smooth and pristine inner surface without crack at all microwave power outputs of 300, 450, 600, and 850 watts. Although the green ceramic moulds demonstrated an average flexural strength of 3.983 MPa, axial cracks were observed in these moulds under all microwave power conditions when HYFILL B289 S wax was used. This is attributed to the wax's higher melting point, which enables it to maintain structural integrity for a longer period and allows for greater expansion before undergoing thermal degradation. The variation in thermal expansion of both waxes was validated by strain gauge experiments, which concluded that cracks formed only on the HYFILL B289 MOD S moulds.

1. INTRODUCTION

Investment casting (IC) is widely known as a flexible manufacturing technique for producing intricate, thin, near-net shape products with a fine surface finish, leading to time and cost savings [1, 2]. The geometry of the final part of the required cast directly depends on the characteristics of the pattern. Therefore, selecting pattern material and addressing its thermal behaviour is crucial to prevent ceramic shell cracking during heating [3]. Wax is widely used due to its low cost, adjustable properties, easy assembly, and low melting point [4]. The modelling wax pattern for investment casting is an intricate blend of vegetable, mineral, and synthetic waxes combined with resins, fillers, additives, and occasionally water [5, 6]. Typically, wax performance is evaluated through various criteria, including melting point, expansion, ash content, phase separation tendency, mechanical traits such as cavitation and strength, as well as attributes such as plasticity, viscosity, and welding behavior [7, 8].

In investment casting, dewaxing is an essential stage, crucial for creating space within the ceramic mould to accommodate the molten metal [4]. This process is achieved by heating the ceramic mould. Moreover, the heating process must be rapid to minimize wax expansion, thereby avoiding cracking and dimensional changes in ceramic moulds [9, 10]. There are several dewaxing methods; however, the flash-fired and autoclave methods are the most commonly used traditional methods [11]. In modern industries, eco-friendly alternatives like microwave heating replace energy-intensive conventional systems for efficient dewaxing [12]. Microwaves generate heat by interacting with the unique dielectric properties of material [13, 14]. Microwave heating offers uniform heating, reduced processing time, and improved product quality [15]. Efficient microwave absorption depends on a material's dielectric properties [16, 17]. The dielectric constant (ε') represents polarization and microwave absorption, while the dielectric loss factor (ε'') indicates the absorbed energy conversion into heat. The dielectric loss tangent ($\tan \delta$), which is the ability of the material to heat up when exposed to microwaves, represents the ratio ($\varepsilon''/\varepsilon'$) [18]. Materials with ε'' below 0.01 are microwave transparent, those at 0.01 to 5 are effective absorbers, and those above 5 reflect microwave radiation [19, 20].

Limited literature has discussed factors influencing, benefits, and applications of microwave energy in investment casting. Efforts to reduce dewaxing time, including using microwave hybrid heating by adding: activated carbon [21, 22], nano alumina [23], during ceramic mould and pattern wax preparation, resulted in some success. Therefore, a more comprehensive investigation is needed in this area. This work aims to evaluate the effects of thermal and dielectric characteristics of the wax and green mould on the microwave dewaxing process in two different types of casting wax. SIVUCH L1203, a new wax material, has the potential to replace the current HYFILL B289 MOD S wax, but its performance has not been well assessed & reported in the literature. However, a comprehensive understanding of wax properties is indispensable for enhancing the precision casting process.

2. DESIGN AND METHODOLOGY

2.1. Materials

The patterns were made using two different types of wax, HYFILL B289 MOD S wax and SIVUCH L1203 wax supplied by REMET Co. Ltd., UK, and LIANG LINN ENTERPRISE Co. Ltd., Taiwan, respectively. The composition and properties of both types (MSD sheet) are presented in Table 1. Colloidal silica (SiO_2) was used as a binder material (BINDZIL-AkzoNobel Asia, Pte. Ltd, Taiwan). Zirconium silicate powder (ZrO_2-SiO_2) of 74μm used as refractory ceramic for slurry (ENDEKA Ceramics Co., Ltd, Spain). Aluminum-silicate (Al_2O_3-SiO_3) was provided in two types, fine and coarse, in particle sizes range of (300-400 μm) and (700-800 μm), respectively, supplied by PRESIDENT Co. Ltd., Taiwan.

Table 1. MSD sheet, the composition percentages and properties of both pattern waxes used.

Type of pattern wax	Compositions	Softening point	Melting point	Viscosity (cP)
HYFILL B289 MOD S wax	Paraffin, microcrystalline, 30% polymers, 0.5% styrene and resins	67 to71 ˚C	70 to 84 ˚C	400 to 600 at 100 ˚C
SIVUCH L1203 wax	40% paraffin, 27% dammar resin, 11% Eva polymer, 8% ceresin, 7% synthetic resin and 3% beeswax, 1% microcrystalline	58 to 60 ˚C	60 to 70 ˚C	300 to 340 at 70 ˚C

2.2. Wax pattern preparation procedure

The pattern shape and dimensions of the two waxes are illustrated in Figure 1(a). LM6-aluminium mould that serves as a mould for wax was designed from two halves sections for easy pattern removal as shown in Figure 1(b). A circular stepped-shaped pattern specimen was designed to allow the investigation of the effect of various thicknesses on the casting behavior; besides, easy handling of patterns. In pattern production, the two halves of the mould were firmly clamped together using a press. Subsequently, the investment wax inside a container was heated on an electric hot plate until it reached a complete melting point of 70 to 110 ˚C. After the wax fully melted, it was poured into the mould and left to solidify at room temperature. Then, the wax pattern was carefully removed by opening the mould in two halves.

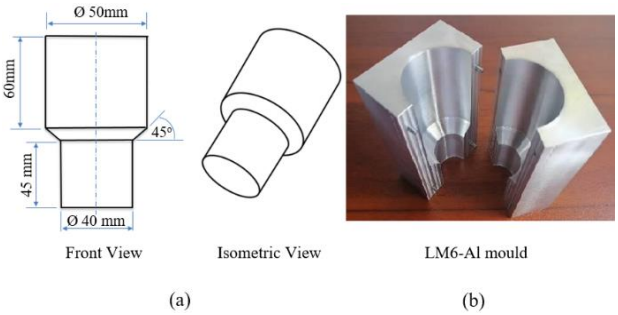

Fig. 1. (a) Shape and dimensions of pattern and, (b) LM6- aluminium mould.

2.3. Ceramic mould preparation

The ceramic mould shell was fabricated by dipping the wax pattern into the ceramic slurry, and stucco (Al_2O_3-SiO_3) was sprinkled over it and left to dry. This process was repeated several times to obtain the required mould thickness. The slurry was created by combining ZrO_2-SiO_2 powder with a colloidal silica binder in a 70% to 30% ratio. The specifics of the shell construction layers are outlined in Table 2 and illustrated in Figure 2.

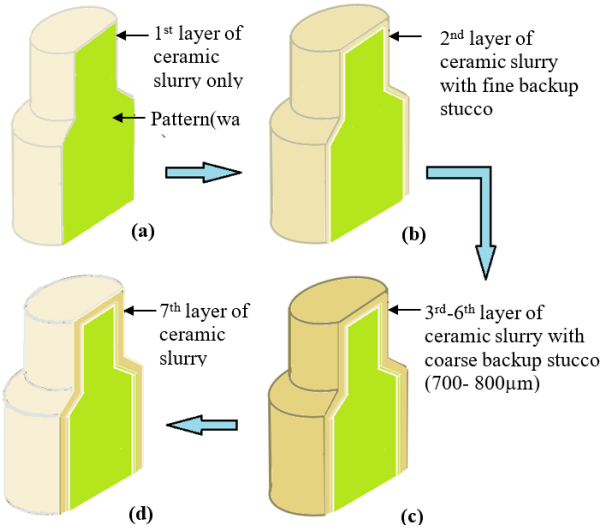

Fig. 2. Sequence of ceramic slurry and stucco application for preparing ceramic shell mould.

Table 2. Details of green mould shell construction layers.

Coating layer	Composition	Slurry Viscosity (sec)	Dipping time (sec)	Drain time (sec)	Dry time (hour)
1st layer (primary)	Slurry	26-28	25-30	40-60	4
2nd layer (backup 1)	Slurry + fine stucco	20-22	25-30	40-60	3
3rd to 6th layer (backup 2-5)	Slurry + coarse stucco (for each layer)	20-22 (for each)	25-30 (for each)	40-60 (for each)	3 (for each)
7th layer (seal)	Slurry	26-28	25-30	40-60	24

Note. Zahn cup 4 was used to measure the slurry viscosity (Zahn seconds) [24].

2.4. Thermal and dielectric testing procedures

The thermogravimetric analysis test (TGA) was employed to measure the weight loss of two pattern wax types as a temperature function. TGA (Mettler Toledo, SDTA851e) was used at a constant heating rate (10 ℃ /min) under nitrogen (N_2) atmosphere, and the waxes were heated in the range of 27 ℃ to 500 ℃. The test is performed by carefully weighing a small wax sample and placing it in a crucible, then inserting it into the TGA instrument. The process involves gradually applying heat while continuously observing the sample's weight. As the temperature rises, the real-time reduction in weight of the wax sample is recorded, attributable to its thermal decomposition. The differential thermal analysis test (DTA) was employed to identify phase transitions, endothermic and exothermic reactions, and melting points. In the process, the wax to be tested and reference material are placed in separate crucibles side by side. The instrument's temperature range and rate are set, and as temperature changes, ΔT is measured.

The dielectric properties for the green ceramic mould shell and the two types of waxes used in this study were measured using the open-ended coaxial probe method in conjunction with the Agilent Technologies vector network analyzer (VNA-85070E). The dielectric properties measured were dielectric loss tangent ($t\,a\,n\ \delta$) and dielectric loss factor (ε''). The measurement was carried out in the range of 0.2-15 GHz and at a temperature of 20 ℃.

A 3-point bend test was used to determine green shell strength in this work following the popular standard test method (ASTM C1161). The samples were loaded onto a tensile testing machine as shown in Figure 3. A load was applied at a constant rate (1 mm/min) until sample failure. The flexural strength (σ_{max}) [MPa] of the sample was calculated using the equation (1) [25]. Flat rectangular bars were prepared in dimensional of length of 90mm, width of 10mm and thickness of about 7.0 ± 0.5 mm according to the international standard designation C1161 [25, 26].

$$\sigma_{max} = \frac{3F_{max}L}{2wh^2} \quad (1)$$

Where: F_{max} is the fracture load applied (N), L, w and h are the length, width and thickness of the test sample (m), respectively.

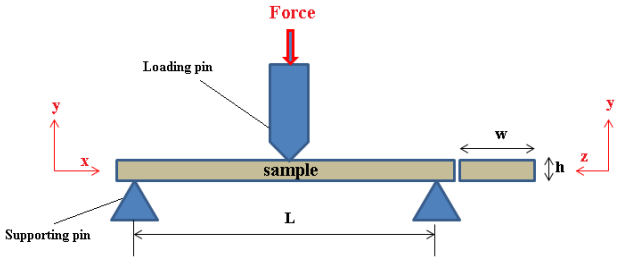

(a)

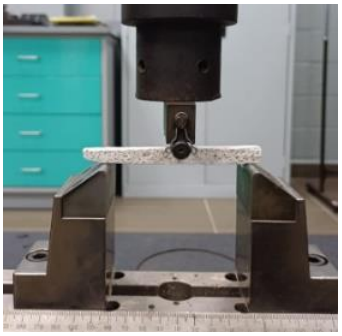

(b)

Fig. 3. 3-point bending test (a) schematic diagram, (b) real test.

2.5. Dewaxing test

A 28-litre Samsung commercial microwave oven with a multi-mode applicator was used to melt the wax pattern from the ceramic mould shell, as shown in Figure 4.

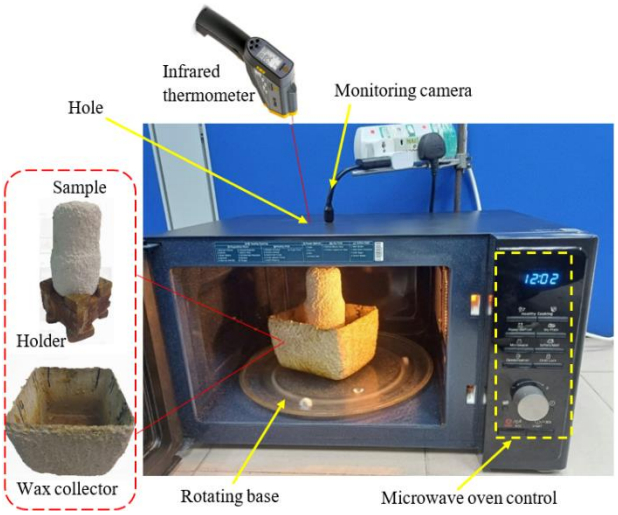

Fig. 4. Experimental set-up for the microwave dewaxing process.

The dewaxing process was performed under ambient environmental conditions and the process was evaluated at varying power of 300W, 450W, 600W, and 850W and operated at 2.45GHz. A Wi-Fi USB mini camera was mounted on the top of the microwave cavity to monitor the process and determine the real-time dewaxing process inside

the microwave oven. A comparison was made between the results to analyze the effects of varying microwave power on dewaxing. The temperature of the ceramic moulds was monitored continuously during the dewaxing process stage by using an infrared thermometer, as depicted in Figure 4. Measurements were conducted at the top of the mould due to its convenient accessibility through an 8 mm hole at the top of the microwave cavity.

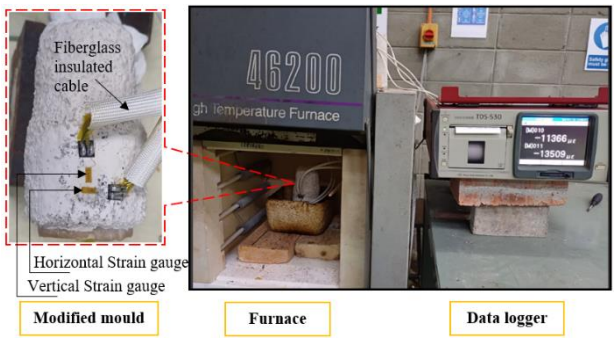

Fig. 5. Arrangement of the strain gauges dewaxing test (a)test sample and, (b)muffle furnace.

To evaluate the effect of the waxes on the mould shell, two geometrical moulds, constructed identically using different types of wax, were assessed for thermal strain. For this purpose, vertical and horizontal high-temperature strain gauges were installed on their outer surfaces. These gauges, connected to a data logger through fiberglass-insulated cables, allowed for precise monitoring of thermal strain, as illustrated in Figure 5(a). Due to the impact of microwaves on the strain gauges, which could not withstand such conditions, the dewaxing process was conducted inside a muffle furnace instead of a microwave, as shown in Figure 5(b). The data logger was recorded between the furnace temperature of 70 to 200 ˚C.

3. RESULTS AND DISCUSSION

3.1. Thermogravimetric analysis (TGA & DTA)

The TGA and DTA curves of both waxes namely HYFILL B289 MOD S wax and SIVUCH L1203 wax, were shown in Figure 6. From TGA analyses, it is found that the apparent weight loss curve of HYFILL B289 S wax indicates an onset of weight loss at approximately 176 ˚C and continues until 410 ˚C as the first stage, with a loss rate of about 40% of the total weight. The sample entered the weight loss stage up to 490 ˚C. At this point, the entire sample completely burn-off due to its organic [27]. On the other hand, the SIVUCH L1203 wax started the weight loss stage at 142 ˚C (34 ˚C lower than HYFILL B289 S wax) and completely burn-off at 420 ˚C. Both waxes, however, showed an identical thermocompatibility and melting peaks, respectively.

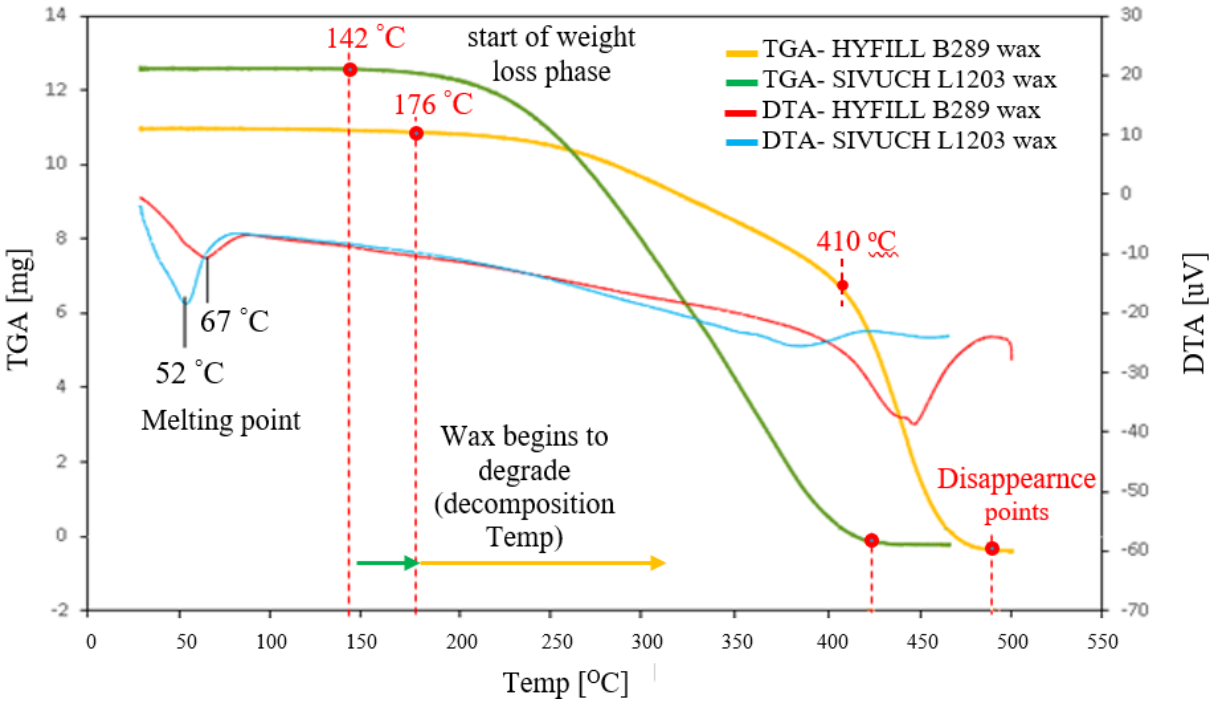

Fig. 6. TGA and DTA results of the HYFILL B289 MOD S wax and SIVUCH L1203 wax.

From DTA curve, it was identified that the HYFILL B289 S wax had two endothermic peaks; the first endothermic peak emerged at 67 ˚C with a fairly low peak value, presumably as a result of HYFILL B289 S wax's phase change (solid to liquid, melting started). The second peak appeared at the end stage of wax decomposition at the temperature of 450 ˚C. SIVUCH L1203 wax however only had one sharp absorbing peak at 52 ˚C, indicating better heat absorption capability and low melting point compared to HYFILL B289 S wax [28].

The TGA and DTA plots collectively demonstrate that HYFILL B289 wax can endure higher temperatures before significant thermal degradation occurs, as evidenced by its higher decomposition temperature. This resilience indicates that HYFILL B289 maintains its structural integrity for a longer period during thermal expansion [29]. Moreover, its higher melting point suggests a greater potential for thermal stability before transitioning to the liquid phase, allowing for considerable expansion as the temperature nears the melting point [30].

3.2. Dielectric properties analysis

Dielectric tests measured at 2.45GHz revealed that the dielectric properties of ceramic mould and HYFILL B289 S wax are almost similar, as shown in Figure 7. Thus, both ceramic mould and wax absorb heat at almost the same rate during the dewaxing process. In contrast, SIVUCH L1203 wax displays dielectric properties that are four times greater than those of HYFILL B289 S wax and green ceramic mould. Notably, a high dielectric loss factor in a material indicates its proficiency in dissipating substantial energy as heat when subjected to an alternating electric field [31, 32]. As such, SIVUCH L1203 wax, characterized by a higher dielectric loss factor, exhibits an enhanced capacity to absorb microwave energy and efficiently convert it into heat. This phenomenon results in an elevated loss tangent, which is the ability of the wax material to heat up when exposed to microwaves [33]. The types and concentrations of resins and polymers play a crucial role in influencing the dielectric properties of wax, primarily by enhancing its dielectric constant and insulation capabilities [34, 35]. Among these, the content of damar resin is particularly significant in boosting dielectric properties. Consequently, the superior dielectric performance of SIVUCH L1203 is attributed to its higher damar resin content (27%) [36, 37].

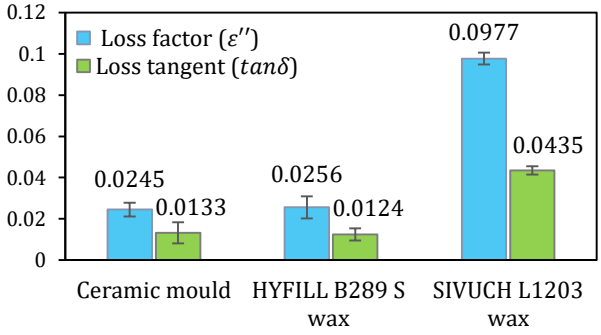

Fig. 7. Dielectric properties comparison between ceramic mould, HYFILL B289 S wax, and SIVUCH L1203 wax.

3.3. Flexural strength analysis of green mould

Table 3 displays the results of the flexural extension and maximum load (N) for three specimens. The thickness of the samples shows slight variation, ranging from 0.00735 m to 0.00765 m. This minor difference in thickness correlates with the flexural strength of the samples also varies, with values from 3.905 MPa to 4.101 MPa. The study showed superior performance in green flexural strength, averaging 3.982 MPa across the three samples. Thus, the ceramic shell presents heightened load-bearing capacity and enhanced resistance to shell wall cracks when removing the wax pattern [38, 39].

Table 3. Flexural strength analysis of green mould.

Sample No	Length [m]	Width [m]	Thickness [m]	Flexural load [N]	Flexural strength [MPa]
1	0.09	0.01	0.00735	15.63	3.905
2	0.09	0.01	0.00765	17.78	4.101
3	0.09	0.01	0.00754	16.37	3.941
Average					3.982

3.4. Post-dewaxing analysis

3.4.1. Effect of microwave power levels on the dewaxing process

In industrial operations, determining the appropriate power level of microwaves depends on various factors, including the material type [40], desired heating or curing rate [41], and specific equipment used [42]. This study used four microwave power levels (300W, 450W, 600W, and 850W) during the dewaxing process and evaluated mould integrity after each process. Table 4 illustrates the temperature progression during the dewaxing process using SIVUCH L1203 wax and at various microwave power levels over time. It is evident that as the microwave power increases, the rate at which temperature rises also accelerates. For example, at 2 minutes, the temperature at 300 W is 33.5 ˚C, whereas at 850 W, it reaches 58.7 ˚C. This trend continues throughout the process, with the temperatures at higher power levels consistently surpassing those at lower power levels. Dewaxing is completed at 18 minutes for the 850 W setting, while it took about 31 minutes to complete dewaxing at 300 W. A notable 39% decrease in dewaxing time was observed when the microwave power was increased from 300 W to 600 W. However, the difference in dewaxing time between 600 W and 850 W was minimal, approximately 8%. At these higher power levels, the waxes were fully removed from the mould at nearly the same time.

Table 4. Temperature distribution during the dewaxing Process at various microwave heating power – SIVUCH L1203 wax.

Dewaxing time (min)	Temperature along the dewaxing process at various microwave power.			
	300 W	450 W	600 W	850 W
2	33.5	41.4	51.6	58.7
4	41.8	48.7	67.3	83.3
6	48.0	56.7	84.9	109.2
8	55.5	64.5	100.7	123.0
10	64.2	71.3	109.0	129.1
12	71.5	82.4	115.0	129.9
14	74.2	94.7	123.4	131.6
16	83.0	108.7	128.6	134.2
18	95.6	114.0	129.0	133.7
20	100.5	115.0	129.7	
22	112.6	123.1		
24	116.6	130.5		
26	125.3	135.0		
28	131.2		Completed dewaxing	
30	134.5			
32	136.8			

The plots in Figure 8(a), show temperatures versus time during the dewaxing process of moulds using microwave power of 600W. While Figure 8(b) shows the thermal image of the temperature distribution of the mould after the dewaxing process. The experimental results reveal that the maximum temperature reached during the 19 minutes heating period was approximately 129°C. This observed temperature drop is attributed to the low dielectric loss properties of the ceramic mould, which results in a slow heating process. It is acknowledged that the heating rate and maximum achievable temperature depend on the dielectric properties of the materials involved [43]. The thermal image indicates the uniform temperature distribution, with only a few hot spots. Table 5 summarises the effects of microwave power on the outer ceramic mould integrity and dewaxing time after the dewaxing process using two types of wax.

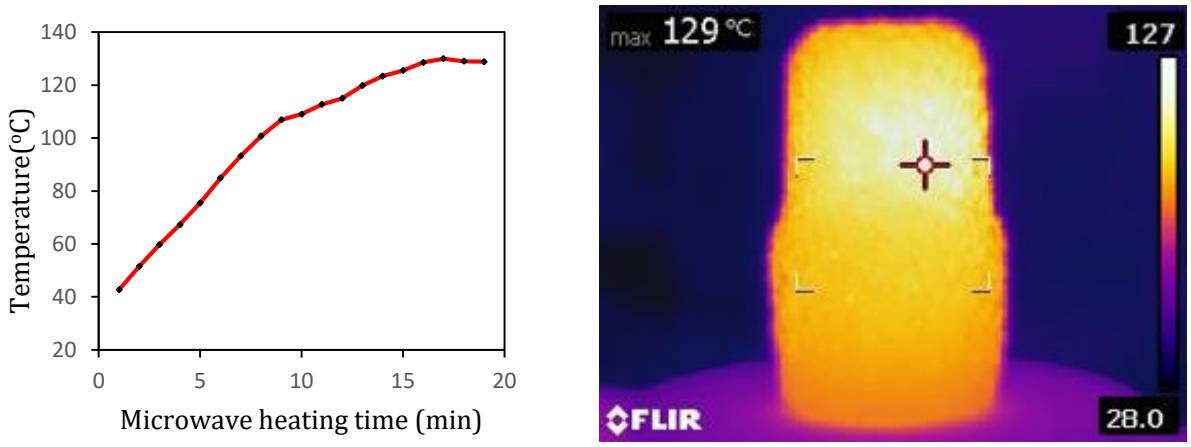

(a) (b)

Fig. 8. Temperature distribution analysis during dewaxing process at 600W microwave power (a) Temperature against time plots, (b) Thermal image after dewaxing process completed.

Table 5. Crack observation on ceramic mould surface after dewaxing process with various microwave power.

Microwave power (Watt)	Type of wax			
	HYFILL B289 S wax		SIVUCH L1203 wax	
	Dewaxing time (minute)	CRACK	Dewaxing time (minute)	CRACK
300	32.50	Yes	31.00	No
450	26.00	Yes	24.50	No
600	20.50	Yes	19.00	No
850	19.00	Yes	17.50	No

The selection of 600 watts of microwave power for the dewaxing process is a decision rooted in both efficiency and safety considerations. One of the primary reasons for this choice is the observation that there is no significant difference in wax removal time between used 600 W and 850 W. The experiments have shown that while increasing the microwave power can reduce the dewaxing time, the reduction beyond 600 watts is marginal. Furthermore, at high microwave power, rapid heating occurs, causing ceramics to become susceptible to sudden temperature changes, which can result in thermal shock and fracture [44]. Conversely, the ceramic material is heated more uniformly at medium power levels. This prevents the hotspots that can occur at high power levels, ensuring that the entire ceramic object or sample reaches the required temperature evenly [45]. Another critical factor to consider is the impact of high temperatures on the life and recyclability of the wax. Elevated temperatures, exceeding the melting point can cause thermal degradation of the wax, leading to a breakdown of its chemical structure, alterations in its thermal properties and linear shrinkage [46]. This degradation reduces the quality and effectiveness of the wax for future use, thereby decreasing its recyclability [47].

3.4.2. Effect of dewaxing process on outer and inner mould shell surfaces

The visual inspection results of the moulds (Table 5) revealed that cracks were observed in all moulds made with HYFILL B289 MOD S wax, across all power levels—300W, 450W, 600W, and 850W, while these defects were absent in the SIVUCH L1203 wax moulds. Consequently, strain gauge measurements were conducted to evaluate the effect of these waxes on the mould shell. In this context, the distribution of the micro-strain depends on how the wax expands and the constraints imposed by the mould geometry [48]. The thermal expansion characteristics curve of the ceramic mould, as measured by horizontal strain gauges, is shown in Figure 9(a). The data reveals a noticeable contrast in the behaviour of the two waxes as heating time progresses. Initially, both waxes

exhibit minimal micro-strain and show linear expansion, indicating stability under low heat. However, as heating progresses, a significant divergence is observed. HYFILL B289 MOD S wax reveals a sudden jump in strain from 184 to 251 με after nearly 160 sec of heating time, continuing to rise steeply, suggesting substantial thermal expansion and potential structural changes. This pattern indicates that, in the first stage, the wax was restricted horizontally by the mould's closed ends, leading to higher pressure and resulting in significant stress on the ceramic mould. With continued heating, the strain curve records a sudden increase (second stage), suggesting the occurrence of a crack in the ceramic mould due to the accumulated pressure from the wax, as illustrated in Figure 10. After this point, the wax continues to expand, increasing the strain further and recording 2733 με at 390 sec. Another significant increase in micro-strain was observed at 334 sec, indicating the occurrence of an additional crack in the mould. In contrast, mould with SIVUCH L1203 wax maintains a relatively stable micro-strain throughout the heating period not exceeding 316 με with the absence of cracks, indicating superior thermal stability, making it more suitable for applications requiring dimensional stability under prolonged heating.

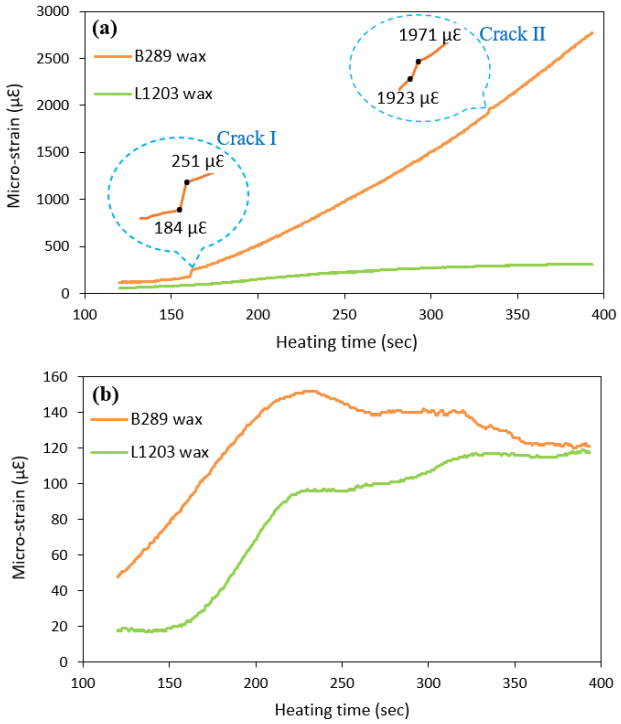

Fig. 9. Micro-strain values of ceramic moulds as a function of heating time for (a) horizontal strain gauges and (b) vertical strain gauges.

Figure 9(b) displays the relationship between vertical strain (με) and heating time (sec) for moulds made with HYFILL B289 MOD S wax and SIVUCH L1203 wax. The open-end configuration of the moulds plays a significant role, allowing the wax to expand more freely towards the open end, thereby reducing constraint and resulting in less pressure and strain. Consequently, the critical difference between these waxes lies in their thermal response. Initially, both waxes exhibit an increase in micro-strain as they are heated, indicating thermal expansion. However, the rate and magnitude of strain differ significantly between the two waxes. The HYFILL B289 wax shows a steeper and more rapid increase in strain, reaching approximately 150 με at around 232 seconds before stabilizing and displaying slight fluctuations. This rapid strain increase suggests that HYFILL B289 wax has a higher thermal expansion force than that of the shell, especially at the first stages of the heating process, leading to greater axial stress on the mould [49]. In contrast, the SIVUCH L1203 wax exhibits a more controlled and less fluctuating strain pattern, peaking at about 118 με around 335 sec before stabilizing. This behaviour allows the mould shell to withstand the force of its thermal expansion better, even when constrained by the closed ends.

It can be seen that the cracks were clearly observed on ceramic mould surfaces that utilized HYFILL B289 S wax. However, an opposite observation was seen when SIVUCH L1203 wax is used in all microwave power. A deep axial crack was observed along the outer and inner surfaces of the ceramic mould, as depicted in Figure 11(a). The width of the crack was most pronounced at the mouth of the mould and gradually diminished towards the apex, eventually becoming imperceptible to the naked eye. This behavior can be attributed to the larger cross-sectional area of the wax near the mouth of the mould compared to the top area. Furthermore, the crack's trajectory was monitored beyond its optical disappearance at the top of the mold using a scanning electron microscope. The analysis revealed that the crack continued to propagate axially, as illustrated in Figure 12. It also seen the remnant of HYFILL B289 S wax after the dewaxing process. In contrast, a clear inner

ceramic mould surface was obtained with SIVUCH L1203 wax which was free from axial crack, as shown in Figure 11(b).

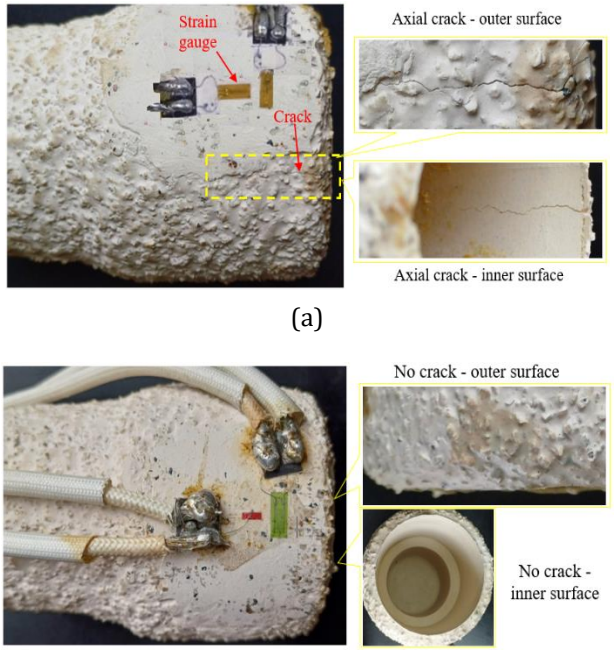

Fig. 10. Inspection results of the ceramic shell after strain gauges dewaxing test (a) Axial crack observed with HYFILL B289 S wax, (b) No crack observed with SIVUCH L1203 wax.

This crack phenomenon is in agreement with the difference in dielectric properties between the two waxes, as well as the disparity in thermal properties between the HYFILL B289 S wax and the ceramic mould material. SIVUCH L1203 wax exhibits about 72% higher dielectric properties than HYFILL B289 S wax, resulting in lower microwave energy absorption of HYFILL B289 S wax compared to SIVUCH L1203 wax. Consequently, an outcome of this disparity induced uneven heating across the wax pattern. These dissimilar temperature distributions, in turn, can trigger expansion phenomena, ultimately giving rise to specific areas marked by heightened stress levels arising from the mechanism of differential thermal expansion. The confluence of non-uniform heating and the ensuing stress concentration fosters the genesis of cracks within the ceramic mould structure [50]. Finally, upon examination of the inner mould surface, residues of HYFILL B289 MOD S wax were detected, whereas the use of SIVUCH L1203 resulted in a clean, smooth surface with no contaminants, as illustrated in Figure 11.

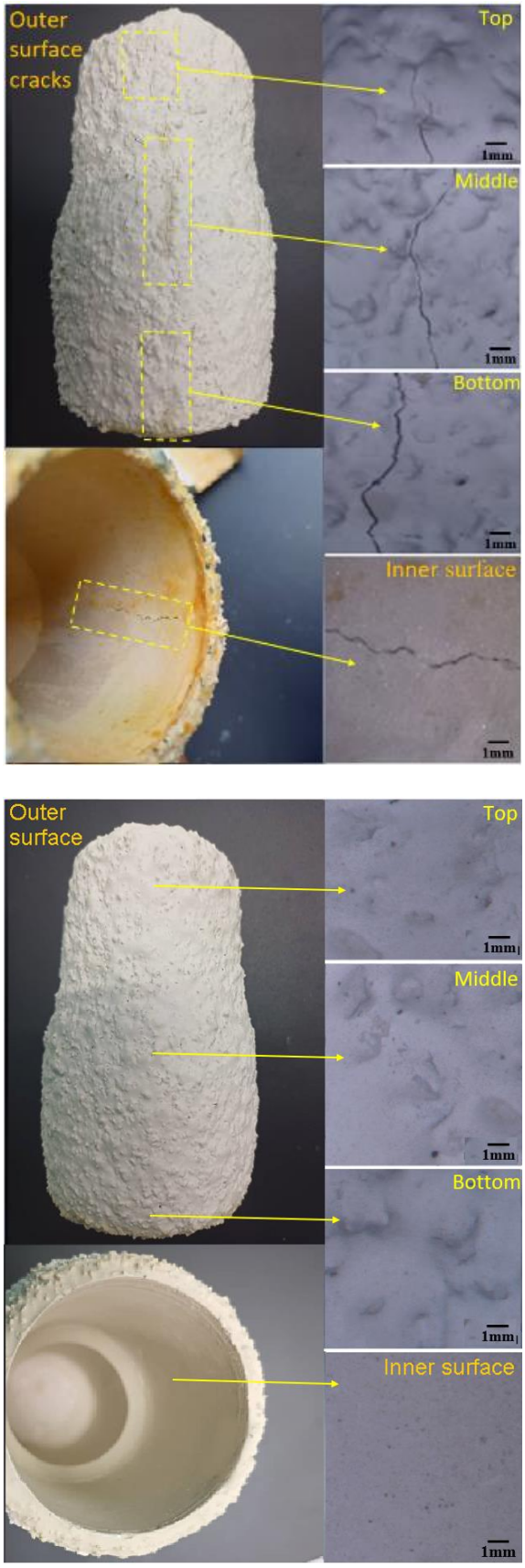

Fig. 11. Optical and micrograph inspection results of the ceramic shell after dewaxing via microwave (a) Axial crack observed with HYFILL B289 S wax, (b) No crack observed with SIVUCH L1203 wax.

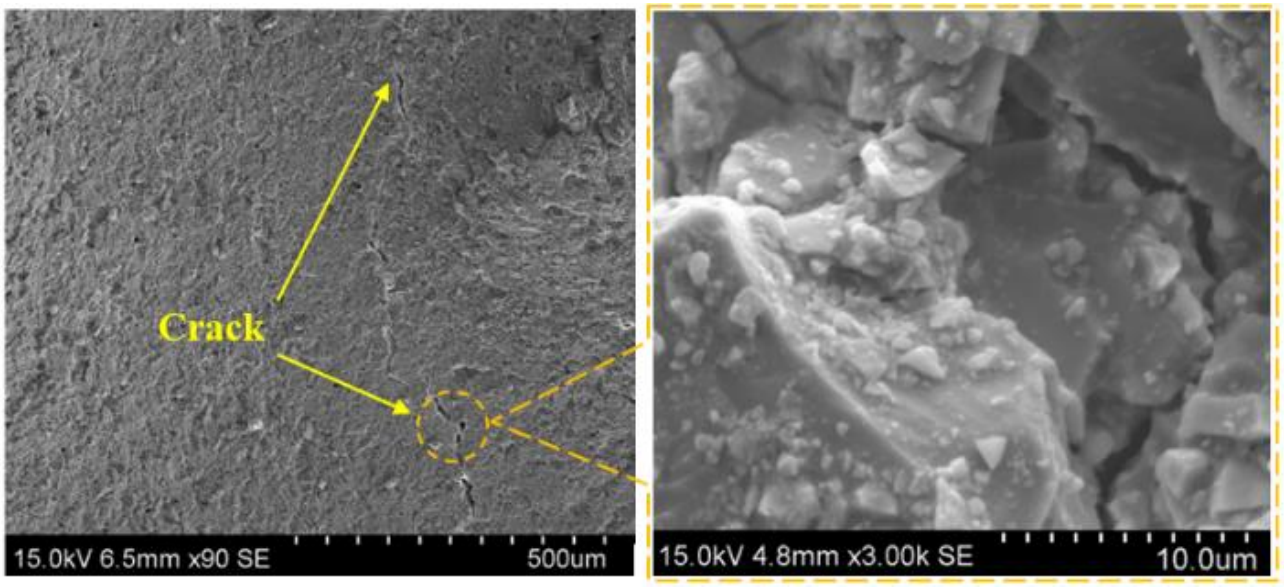

Fig. 12. SEM image of the outer surface at the top of the mould.

4. CONCLUSION

The disparity in thermal properties between the two waxes, particularly in their heat absorption capabilities, leads to SIVUCH L1203 wax exhibiting rapid melting compared to the other type of wax. Consequently, this wax variant avoids generating excessive thermal pressures that could potentially impact the integrity of the ceramic shell during the heating process. Moreover, SIVUCH L1203 boasts insulating properties that enhance its heat absorption capacity by 4 folds compared to HYFILL B289 wax and ceramic mould. This, in turn, expedites the dewaxing process. On the other hand, the elevated melting point of HYFILL B289 wax, coupled with its low dielectric properties, adversely affects the dewaxing time and increases the likelihood of crack formation across all tested microwave power conditions for this wax.

Acknowledgement

The authors would like to acknowledge the Universiti Teknologi Malaysia for research university funding under grant no. 4J641 and Metal Casting Laboratory, Faculty of Mechanical Engineering, UTM. Thanks, are also extended to the Libyan Ministry of Higher Education.

REFERENCES

[1] Y. C. Kao et al., "Computer-Aided Engineering (CAE) simulation for the robust gating system design: improved process for investment casting defects of 316L stainless steel valve housing," *International Journal of Metalcasting*, pp. 1-19, 2022.

[2] C. Morsiya and S. Pandya, "Recent Advancements in Hybrid Investment Casting Process—A Review," *Recent Advances in Manufacturing Processes and Systems: Select Proceedings of RAM 2021*, pp. 817-831, 2022.

[3] W. Everhart, S. Lekakh, V. Richards, J. Chen, and K. Chandrashekhara, "Crack formation during foam pattern firing in the investment casting process," *International Journal of Metalcasting*, vol. 7, no. 2, pp. 7-14, 2013.

[4] S. Pattnaik, D. B. Karunakar, and P. K. Jha, "Developments in investment casting process—A review," *Journal of Materials Processing Technology*, vol. 212, no. 11, pp. 2332-2348, 2012.

[5] T. Piwonka, K. Woodbury, and J. Wiest, "Modeling casting dimensions: effect of wax rheology and interfacial heat transfer," *Materials & Design*, vol. 21, no. 4, pp. 365-372, 2000.

[6] L. Szabó, G. Deák, D. Nyul, and S. Kéki, "Flexible Investment Casting Wax Patterns for 3D-Printing: Their Rheological and Mechanical Characterizations," *Polymers*, vol. 14, no. 21, p. 4744, 2022.

[7] A. S. Sabau and S. Viswanathan, "Material properties for predicting wax pattern dimensions in investment casting," *Materials Science and Engineering: A*, vol. 362, no. 1-2, pp. 125-134, 2003.

[8] H. Wang, S. A. Boyer, M. Bellet, and F. Dalle, "Effects of Wax Components and the Cooling Rate on Crystal Morphology and Mechanical Properties of Wax–Oil Mixtures," *Crystal Growth & Design*, vol. 23, no. 3, pp. 1422-1433, 2023.

[9] J. Harrison, "Additive Manufacturing Assisted Casting Methods for Aluminum," Oklahoma State University, 2022.

[10] C. Yuan, S. Jones, and S. Blackburn, "The influence of autoclave steam on polymer and organic fibre modified ceramic shells," *Journal of the European Ceramic Society*, vol. 25, no. 7, pp. 1081-1087, 2005.

[11] R. Samyal, A. K. Bagha, and R. Bedi, "The casting of materials using microwave energy: A review," *Materials Today: Proceedings*, vol. 26, pp. 1279-1283, 2020.

[12] C. Singh, V. Khanna, and S. Singh, "Sustainability of microwave heating in materials processing technologies," *Materials Today: Proceedings*, vol. 73, pp. 241-248, 2023.

[13] Z. Zeng et al., "Structure, dielectric, magnetic and magnetoelectric coupling properties of xPbTiO3/(1-x) NiFe2O4 composite ceramics," *Processing and Application of Ceramics*, vol. 14, no. 3, pp. 223-230, 2020.

[14] L. Wang et al., "Recent progress of microwave absorption microspheres by magnetic–dielectric synergy," *Nanoscale*, vol. 13, no. 4, pp. 2136-2156, 2021.

[15] N. Sruthi, Y. Premjit, R. Pandiselvam, A. Kothakota, and S. Ramesh, "An overview of conventional and emerging techniques of roasting: Effect on food bioactive signatures," *Food Chemistry*, vol. 348, p. 129088, 2021.

[16] D. Clark, D. Folz, and J. West, "Processing of 5083 aluminum alloy reinforced with alumina through microwave sintering," *Mater. Sci. Eng., A*, vol. 287, p. 153, 2000.

[17] F. T. Joenck, V. B. C. Joenck, J. A. V. D. Carpio, and J. V. S. de Melo, "Self-healing capacity of asphalt mixtures with steel fiber, steel slag and graphite powder, evaluated with microwave induction and fatigue test," *Matéria (Rio de Janeiro)*, vol. 27, no. 4, p. e20220221, 2022.

[18] M. Chen, E. Siochi, T. Ward, and J. McGrath, "Basic ideas of microwave processing of polymers," *Polymer Engineering & Science*, vol. 33, no. 17, pp. 1092-1109, 1993.

[19] H. Pang et al., "The electromagnetic response of composition-regulated honeycomb structural materials used for broadband microwave absorption," *Journal of Materials Science & Technology*, vol. 88, pp. 203-214, 2021.

[20] B. Yahaya, S. Izman, M. Idris, and M. Dambatta, "Effects of activated charcoal on dewaxing time in microwave hybrid heating," *Procedia CIRP*, vol. 26, pp. 467-472, 2015.

[21] Y. Q. Gill, F. Saeed, M. H. Shoukat, M. S. Irfan, and U. Abid, "A study on the dewaxing behavior of carbon-black-modified LDPE–paraffin wax composites for investment casting applications," *Arabian Journal for Science and Engineering*, vol. 46, no. 7, pp. 6715-6725, 2021.

[22] B. Yahaya, S. Izman, M. Idris, and M. Dambatta, "Effects of activated charcoal on physical and mechanical properties of microwave dewaxed investment casting moulds," *CIRP Journal of Manufacturing Science and Technology*, vol. 13, pp. 97-103, 2016.

[23] Y. Q. Gill, M. H. Shoukat, F. Babar, U. Mehmood, and U. Abid, "Fabrication and characterization of PANI-modified LLDPE-paraffin wax blends," *Polymer Bulletin*, pp. 1-16, 2022.

[24] Y. Venkat, K. Choudary, D. Das, A. Pandey, and S. Singh, "Ceramic shell moulds with zircon filler and colloidal silica binder for investment casting of shrouded low-pressure turbine blades," *Ceramics International*, vol. 46, no. 17, pp. 26572-26580, 2020.

[25] S. Pattnaik, "Reduction of Shrinkage and Porosity Defects in Investment Casting," PhD Thesis, Indian Institute of Technology, Roorkee, 2014.

[26] A. Standard, "C1161-13 (2013) Standard test method for flexural strength of advanced ceramics at ambient temperature," *ASTM International: West Conshohocken, PA, USA*, 2013.

[27] P. Nanda, "The Effect of Stucco Sand Size on the Shell Mould Permeability and Modulus of Rupture (MOR)," *Journal of Aeronautical-science and engineering*, vol. 13, no. 1, pp. 5-9, 2018.

[28] R. Buchwald, M. D. Breed, and A. R. Greenberg, "The thermal properties of beeswaxes: unexpected findings," *Journal of Experimental Biology*, vol. 211, no. 1, pp. 121-127, 2008.

[29] D. Rahmalina and R. A. Rahman, "The impact of thermal aging on the degradation of technical parameter of a dynamic latent thermal storage system," *International Journal of Thermofluids*, vol. 19, p. 100401, 2023.

[30] C. Gutiérrez-Blandón, A. Cuadri, A. Tenorio-Alfonso, P. Partal, and F. Navarro, "Rheological and phase behaviour of paraffin wax/bitumen blends with thermal storage characteristics," *Construction and Building Materials*, vol. 401, p. 132826, 2023.

[31] H. Chen, T. Li, Z. Wang, R. Ye, and Q. Li, "Effect of dielectric properties on heat transfer characteristics of rubber materials via microwave heating," *International Journal of Thermal Sciences*, vol. 148, p. 106162, 2020.

[32] J. Xu, T. Yu, D. Han, X. Guan, and X. Lei, "Synthesis of Organic Modified SiC w/PVDF Composite Membrane and Its Dielectric Properties under Low Temperature," *Journal of Wuhan University of Technology-Mater. Sci. Ed.*, vol. 34, pp. 1279-1287, 2019.

[33] K. Huang, X. Yang, H. Zhu, K. Huang, X. Yang, and H. Zhu, "Characterization and Measurement of a Chemical Reaction's Dielectric Properties," *Dynamics in Microwave Chemistry*, pp. 5-40, 2021.

[34] T. Matsukura, H. Iijima, and M. Shimakawa, "Resin composition with high dielectric insulation properties," *Google Patents*, 2016.

[35] H.-Y. Tsai, J.-Y. Chen, H.-H. Shih, C.-L. Li, and W.-H. Liao, "Resin composition with excellent dielectric property," *Google Patents*, 2002.

[36] G. Bhattacharya, "The Dielectric Dispersion of a Few Natural Resins in Non-Polar Solvents," *Indian Journal of Physics*, vol. 18, pp. 192-197.

[37] R. Zakaria and A. Ahmad, "Ionic and thermal conductivity studies of silicone-dammar as a coating resin," in *2012 IEEE Symposium on Business, Engineering and Industrial Applications*, 2012: IEEE, pp. 401-404.

[38] K. Tamta and D. B. Karunakar, "Enhancing mechanical properties and permeability of ceramic shell in investment casting process," *Materials and Manufacturing Processes*, vol. 34, no. 6, pp. 612-623, 2019.

[39] S. Pattnaik, "Influence of sawdust on the properties of the ceramic shell used in investment casting process," *The International Journal of Advanced Manufacturing Technology*, vol. 93, pp. 691-707, 2017.

[40] R. Daminev, "The main factors, influencing the processes in the microwave field," in *IOP Conference Series: Materials Science and Engineering*, 2020, vol. 919, no. 2: IOP Publishing, p. 022043.

[41] G. Link and V. Ramopoulos, "Simple analytical approach for industrial microwave applicator design," *Chemical Engineering and Processing-Process Intensification*, vol. 125, pp. 334-342, 2018.

[42] L. A. Campañone et al., "Microwave heating equipment for the food industry," in *Emerging Thermal Processes in the Food Industry*: Elsevier, 2023, pp. 119-163.

[43] Y. Jiao, J. Tang, S. Wang, and T. Koral, "Influence of dielectric properties on the heating rate in free-running oscillator radio frequency systems," *Journal of Food Engineering*, vol. 120, pp. 197-203, 2014.

[44] X. Shang et al., "Electromagnetic waves transmission performance of alumina refractory ceramics in 2.45 GHz microwave heating," *Ceramics International*, vol. 45, no. 17, pp. 23493-23500, 2019.

[45] T. Garnault, D. Bouvard, J.-M. Chaix, S. Marinel, and C. Harnois, "Is direct microwave heating well suited for sintering ceramics?," *Ceramics International*, vol. 47, no. 12, pp. 16716-16729, 2021.

[46] K. Grzeskowiak, D. Czarnecka-Komorowska, K. Sytek, and M. Wojciechowski, "Influence of waxes remelting used in investment casting on their thermal properties and linear shrinkage," *Metalurgija*, vol. 54, no. 2, pp. 350-352, 2015.

[47] P. Intarapong, J. Preechawong, and M. Nithitanakul, "High valuable wax from multilayer film packaging wastes using solid catalyst via pyrolysis process," *Waste Management*, vol. 186, pp. 205-213, 2024.

[48] E. Barati and J. Akbari, "The effect of injection parameters on dimensional accuracy of wax patterns for investment casting," *Journal of Computational & Applied Research in Mechanical Engineering (JCARME)*, vol. 9, no. 2, pp. 313-322, 2020.

[49] A. O. A. Amhamed, I. Sudin, N. N. Mas' ood, N. M. A. Omar, and W. F. F. W. Ali, "Role of silicon carbide in enhancing microwave hybrid heating and reducing dewaxing time in investment casting," *Materials Today Communications*, vol. 39, p. 108842, 2024.

[50] Y. Liu, L. Jiang, X. Wang, F. Du, and J. Zhao, "Mould heat transfer and friction behavior on the surface of wide and heavy slabs in the presence of longitudinal cracks," *Metallurgical Research & Technology*, vol. 120, no. 3, p. 314, 2023.